Electronic Supplementary Material (ESI) for Journal of Materials Chemistry A.

Electronic Supplementary Information

Trimetal atoms confined in openly accessible nitrogen-doped carbon constructs for efficient ORR

Jingjing Wang,[a] Wenjie Zang,[b] Shibo Xi,[c] Mohammadreza Kosari,[a] Stephen J. Pennycook[b] and Hua Chun Zeng[a]*

[a]Department of Chemical and Biomolecular Engineering, National University of Singapore, Singapore 119260, Singapore

[b]Department of Materials Science and Engineering, National University of Singapore, Singapore 117574, Singapore

[c]Institute of Chemical and Engineering Sciences, A*STAR (Agency for Science, Technology and Research), 1 Pesek Road, Jurong Island, Singapore 627833, Singapore

Table of Contents

Figs. S1 to S13: Page 2 to Page 14

Tables S1 and S2: Page 15

References: Page 16

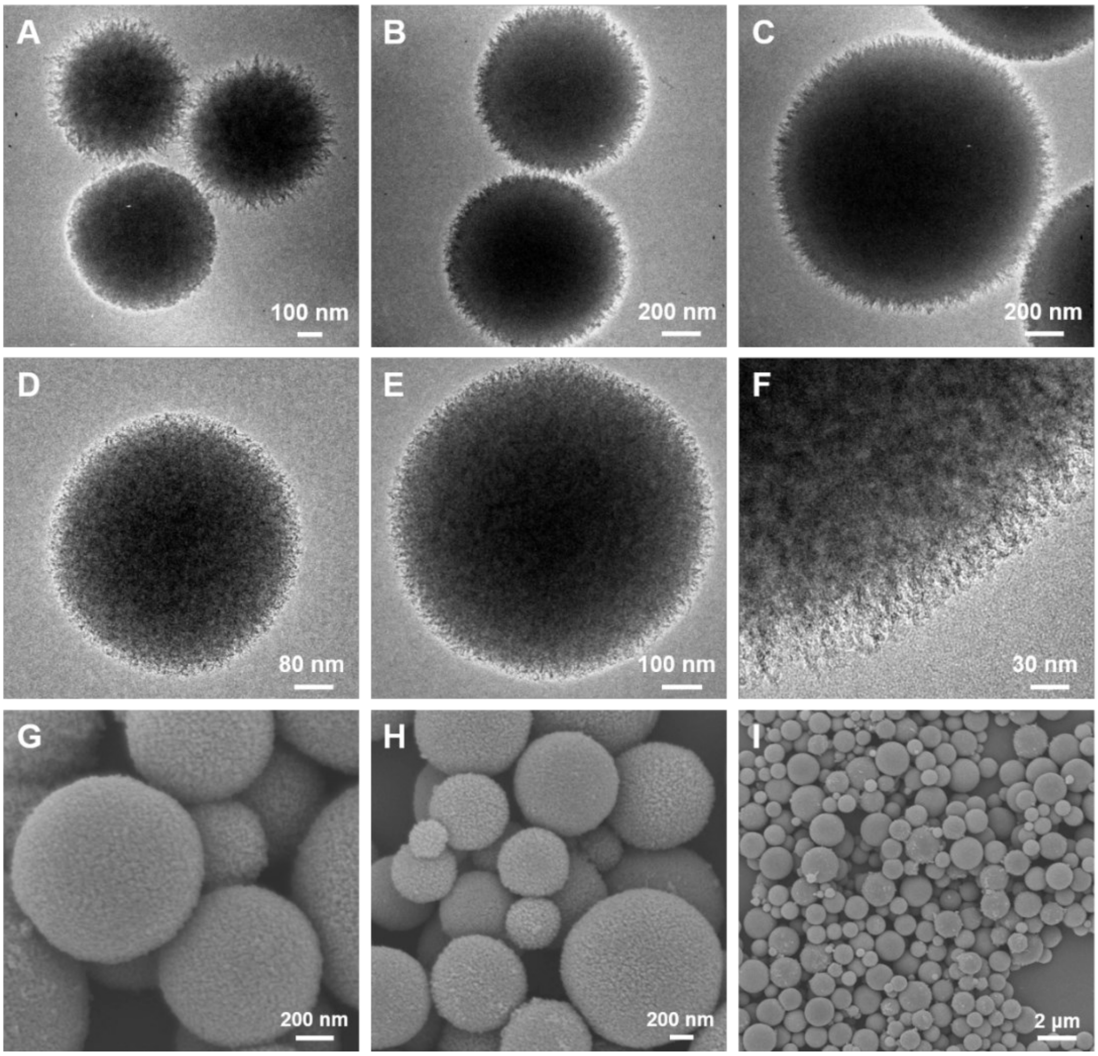

Fig. S1. (A-C) TEM images of amorphous ZIF-90 dandelions, (D-F) TEM images and (G-I) SEM images (at different magnifications) of Zn/NC dandelions (i.e., pyrolysis product of amorphous ZIF-90).

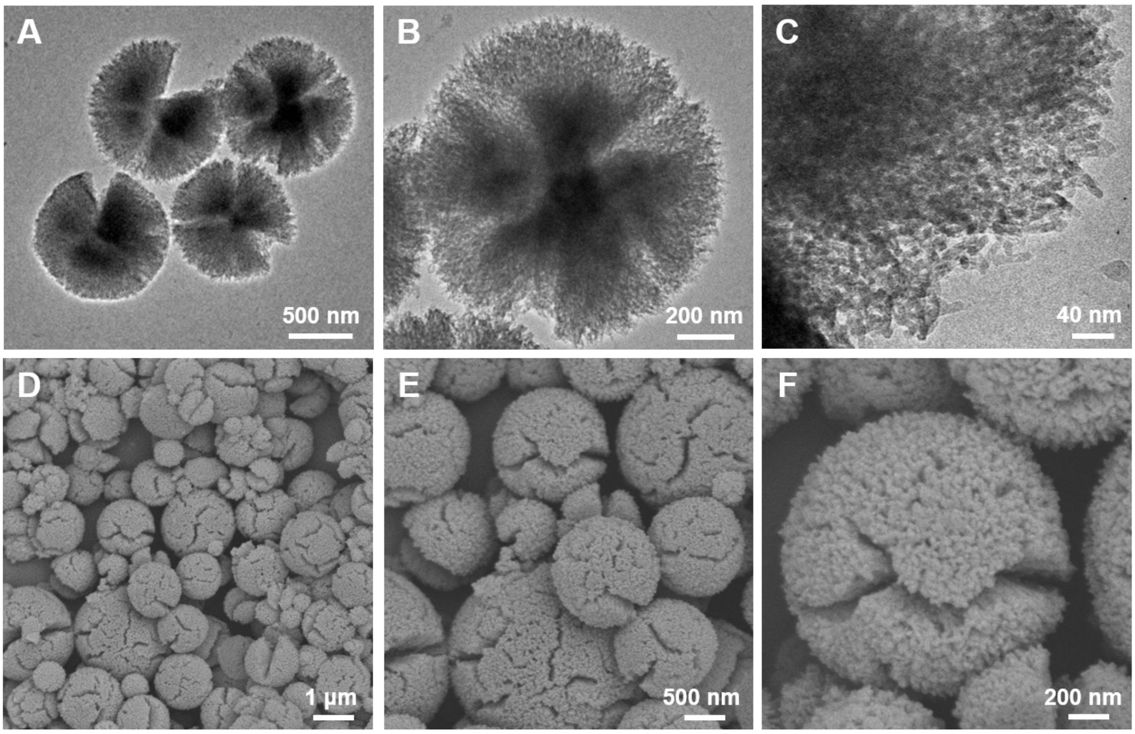

Fig. S2. (A-C) TEM images and (D-F) SEM images of Co, Fe doped ZIF-90 (CoFe-ZIF-90).

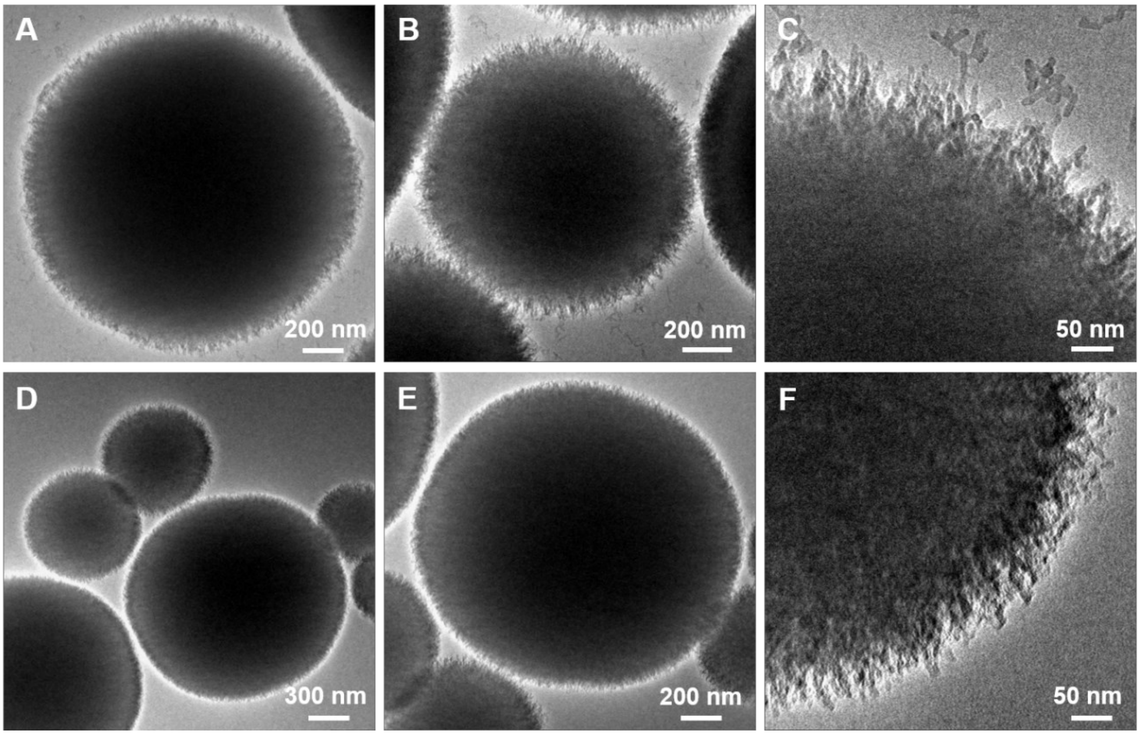

Fig. S3. (A-C) TEM images of Co doped ZIF-90, and (D-F) TEM images of CoZn-NC (i.e., pyrolysis product of Co doped ZIF-90).

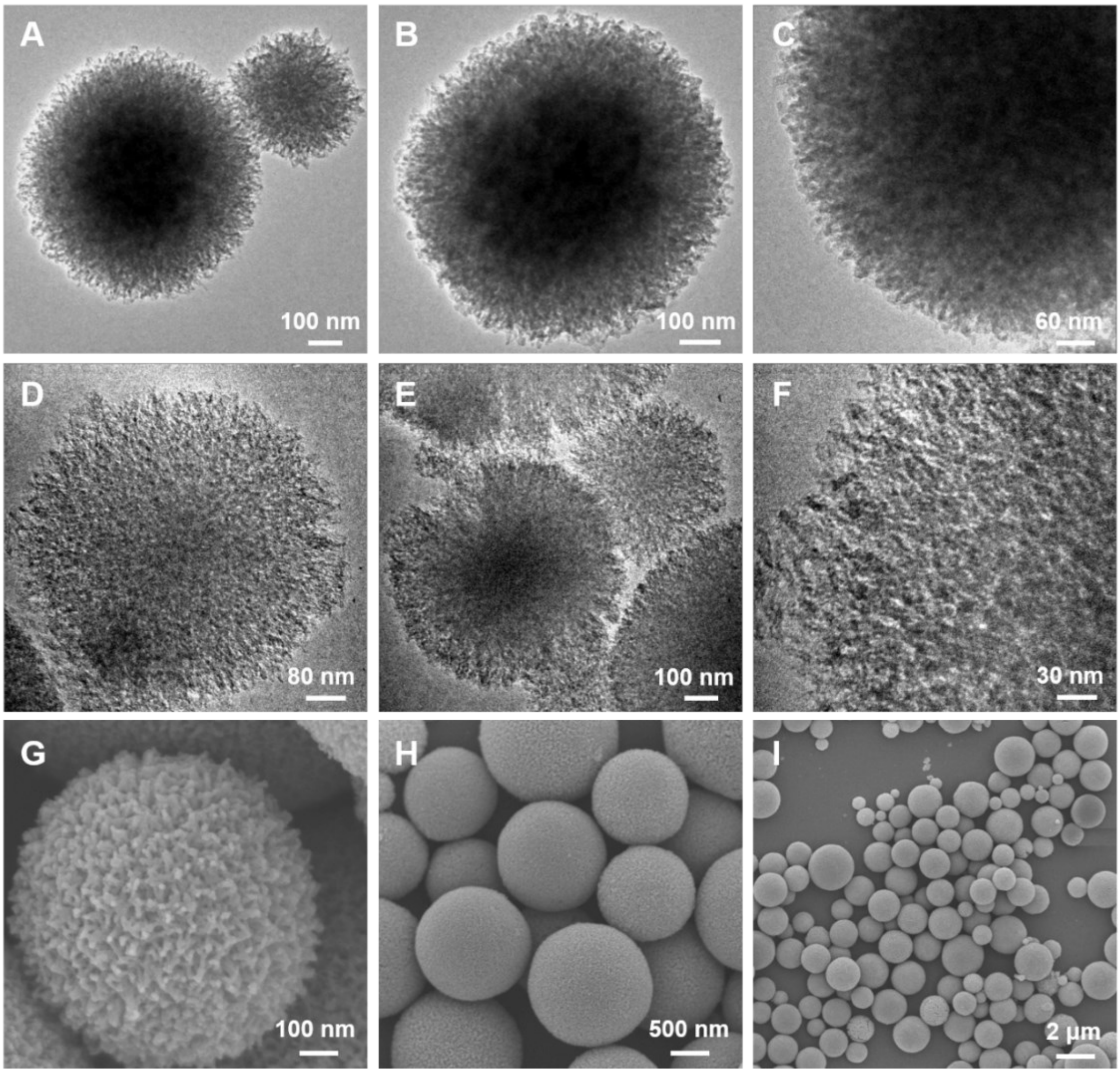

Fig. S4. (A-C) TEM images of Fe doped ZIF-90, (D-F) TEM images and (G-I) SEM images (at different magnifications) of FeZn/NC sample (i.e., pyrolysis product of Fe doped ZIF-90).

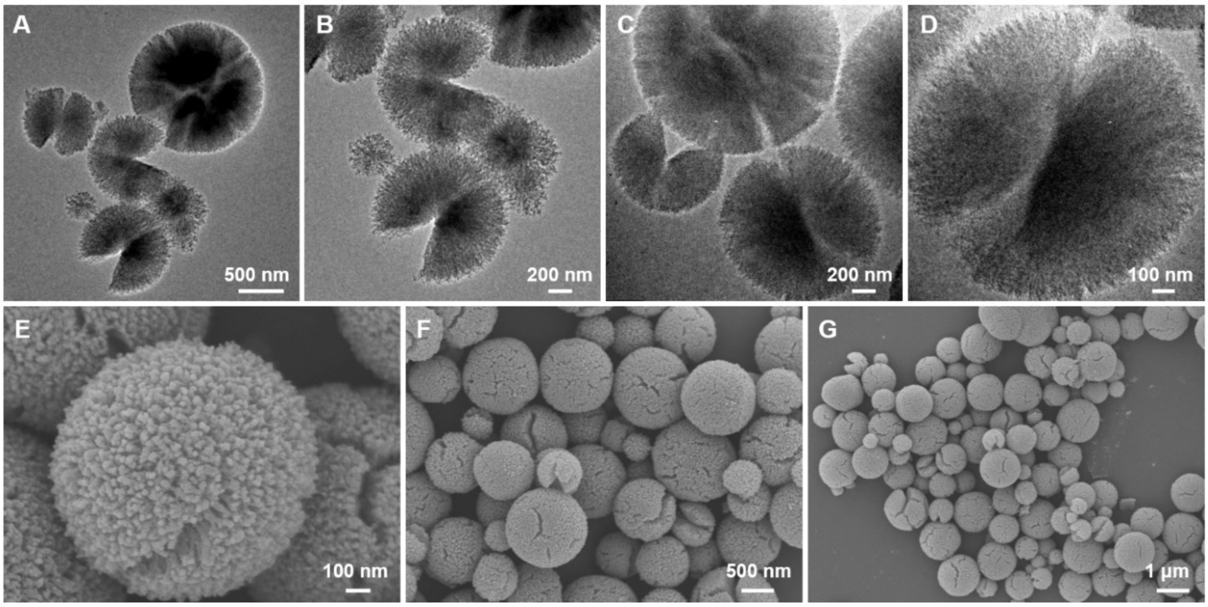

Fig. S5. (A-D) TEM images and (E-G) SEM images (at different magnifications) of $Co_{0.11}Fe_{0.04}Zn$/NC sample.

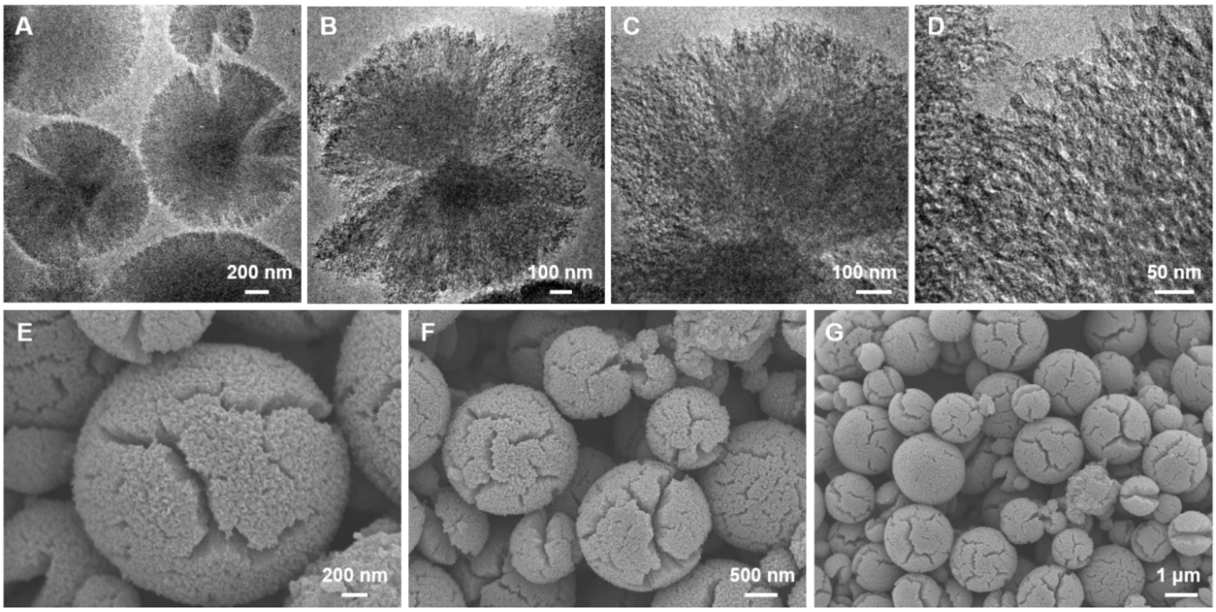

Fig. S6. (A-D) TEM images (at different magnifications) and (E-G) SEM images (at different magnifications) of $Co_{0.34}Fe_{0.04}Zn$/NC sample.

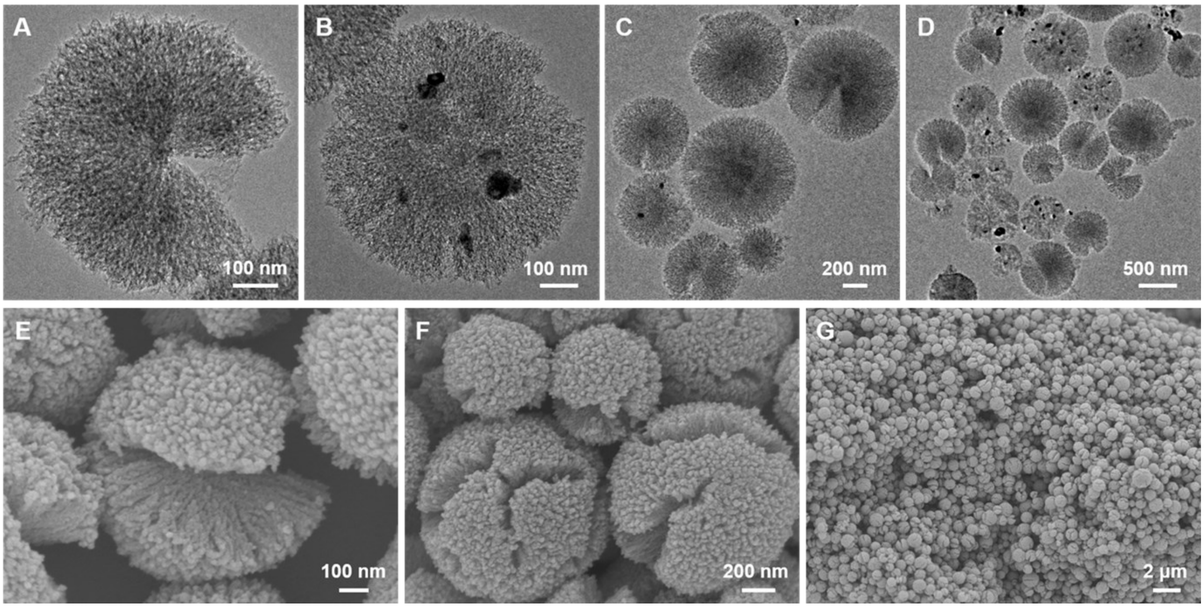

Fig. S7. (A-D) TEM images and (E-G) SEM images (at different magnifications) of $Co_{0.93}Fe_{0.04}Zn$/NC sample.

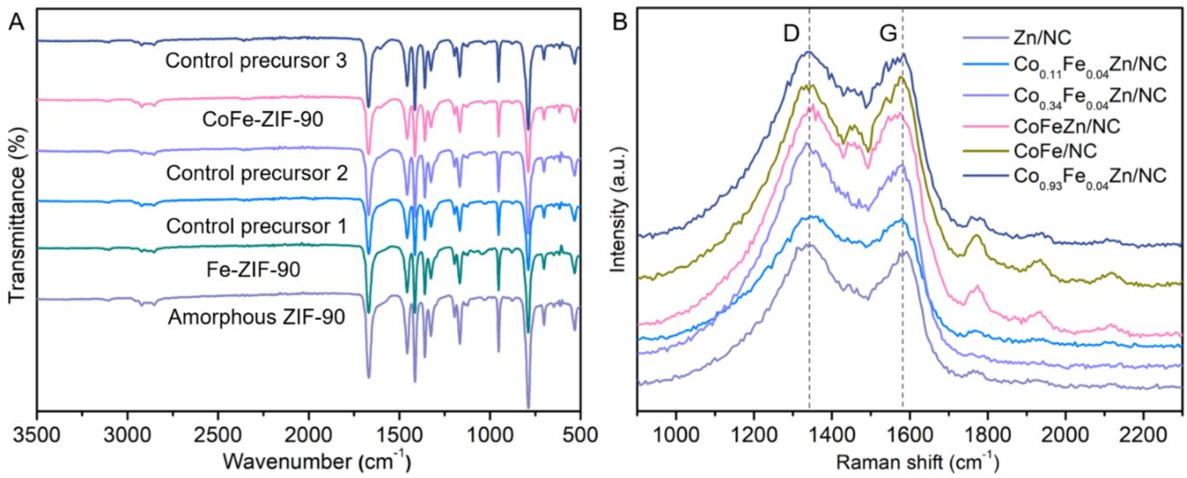

Fig. S8. (A) FTIR spectra of various Co and/or Fe doped ZIF-90 precursors, and (B) Raman spectra of pyrolyzed samples derived from the precursros in (A); detailed synthetic precedures for the control precursors 1, 2 and 3 (with different Co contents) can be found in Experimental Section in the main text.

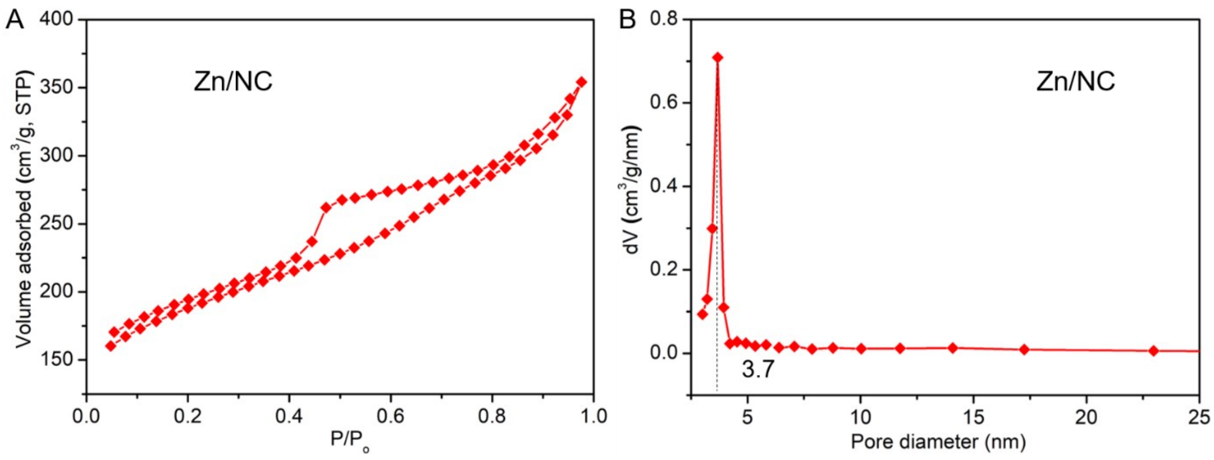

Fig. S9. (A) N_2 adsorption-desorption isotherm and (B) pore diameter distribution of Zn/NC derived from amorphous ZIF-90.

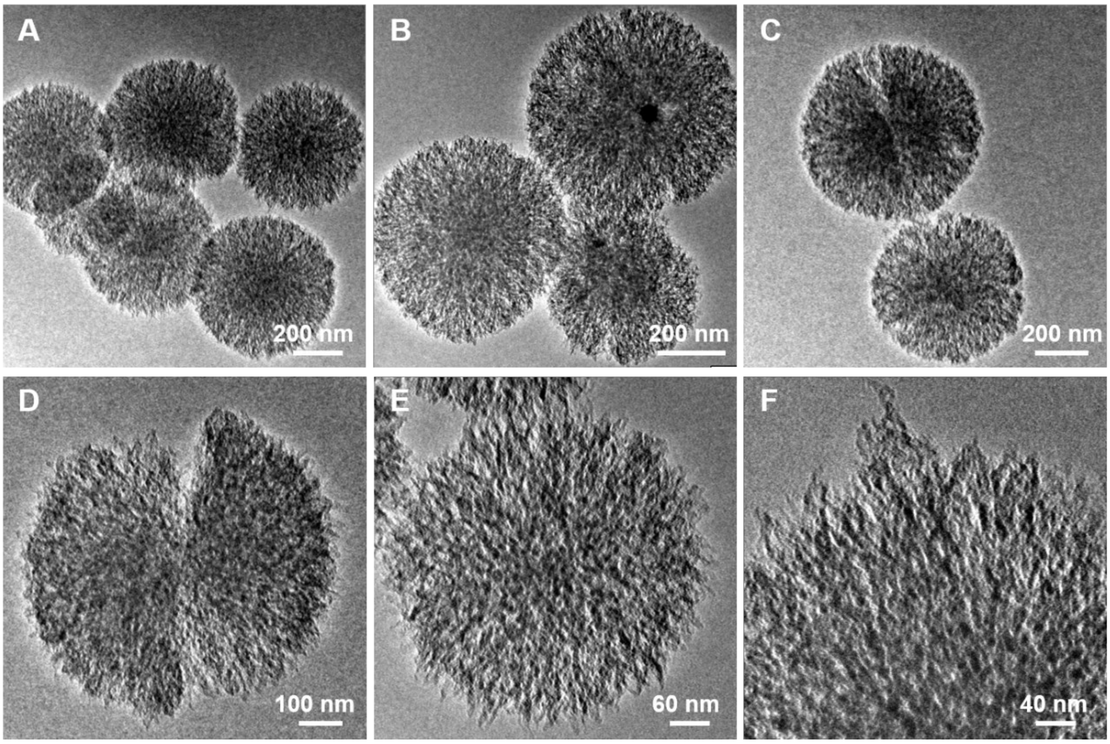

Fig. S10. TEM images of CoFe/NC sample prepared by pyrolysis of Co, Fe doped ZIF-90 at 900 °C for 3 hours.

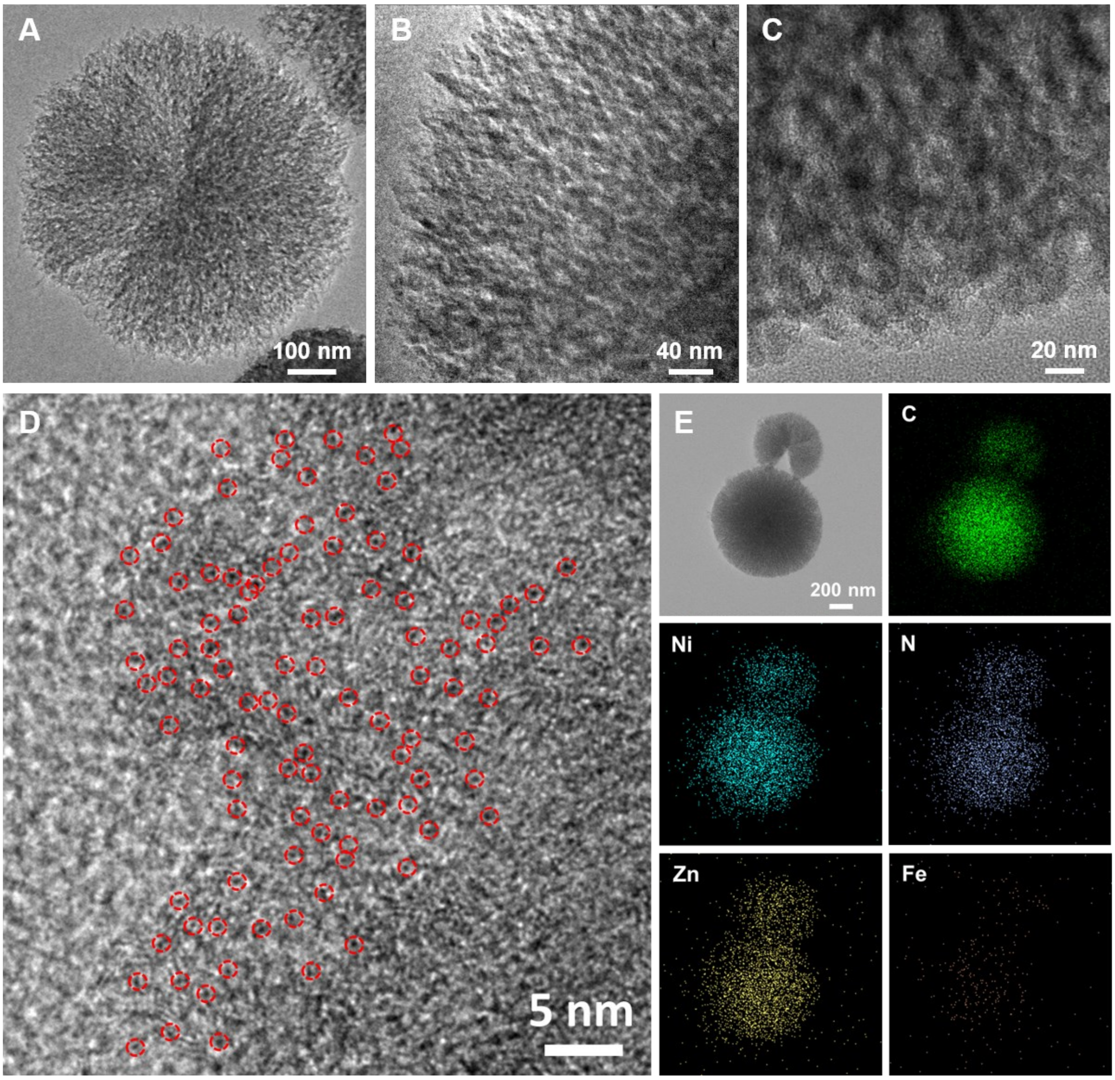

Fig. S11. (A-D) TEM images and (E) EDX elemental maps of NiFeZn/NC sample. In TEM image (D), isolated metal atoms are marked with red circles. The synthesis of NiFeZn/NC is similar to the preparation of other samples, after the formation of amorphous ZIF-90 sample, 10 ml of 0.1 M $Ni(NO_3)_2$ and 4 ml of 0.1 M $Fe(NO_3)_3$ methanolic solution were added and stirred for 3.5 h at room temperature. Then the product NiFeZn-ZIF-90 was collected by centrifuging and washing with ethanol for 3 times. Finally, the dried NiFeZn-ZIF-90 was heated in a tube furnace at 900 ^{o}C for 1 h in Ar atmosphere with a ramping rate of 7.5 °C·min^{-1} to form NiFeZn/NC.

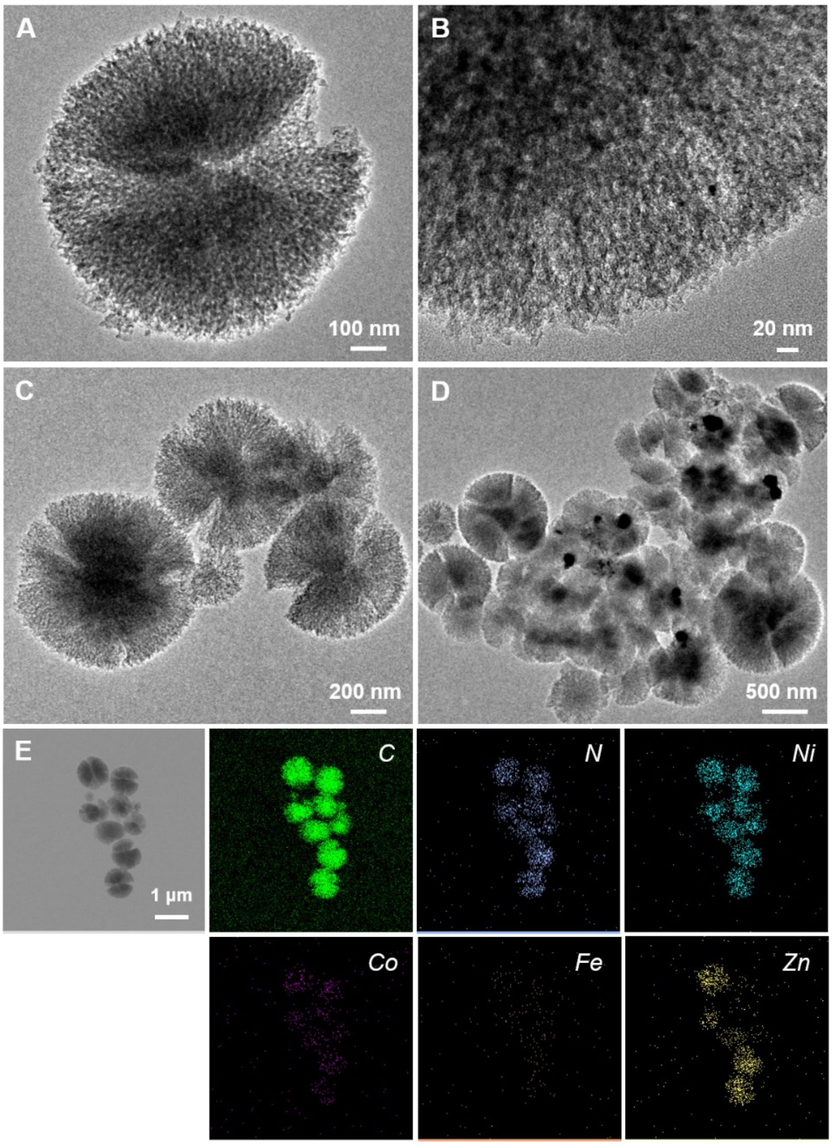

Fig. S12. (A-B) TEM images, (C-D) SEM images, and (E) EDX elemental maps of NiCoFeZn/NC sample. For synthesis of NiCoFeZn/NC, only need to replace the added methanolic solution to 10 ml of $Ni(NO_3)_2$ (0.1 M), 10 ml of $Co(NO_3)_2$ (0.1 M) and 4 ml of $Fe(NO_3)_3$ (0.1 M) methanolic solutions.

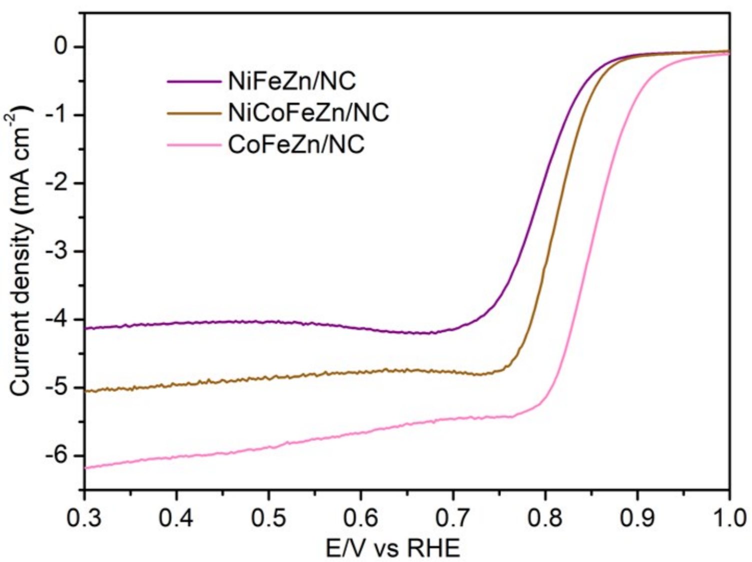

Fig. S13. RDE polarization curves of NiFeZn/NC, NiCoFeZn/NC and CoFeZn/NC sample in O_2-saturated 0.1 M KOH with a sweep rate of 5 $mV \cdot s^{-1}$ and a rotation rate of 1600 rpm.

Table S1. Co K-edge XANES data fitting results of CoFeZn/NC and Co/NC.

Sample	Path	N	R(Å)	σ^2	R factor
Co/NC	Co–N	3.7	1.91	0.0083	0.007
CoFeZn/NC	Co–N	3.6	1.93	0.0070	0.005

Table S2. Comparison of the ORR catalytic performance of our CoFeZn/NC sample to other related high-performance ORR electrocatalysts reported in literatire.

Catalyst	Total metal content (wt%)	Surface area ($m^2 \cdot g^{-1}$)	Pore size (nm)	electrolyte	Halfwave potential ($E_{1/2}$, V)	Limit current density ($mA \cdot cm^{-2}$)	Ref. (year)
Co SAs/N-C	4	1393.7	0.51	0.1 M KOH	0.881	5.6	2016 [1]
(Fe,Co)/CNT		620	0.42	0.1 M KOH	0.954	5.4	2018 [2]
Cu–N–C	20.9			0.1 M KOH	0.869	5.6	2018 [3]
Co, N-CNF	0.27	1170	1.2, 5.2	0.1 M KOH	0.822	5.7	2016 [4]
ISA Fe/CN	2.16			0.1 M KOH	0.900	6.1	2017 [5]
CAN-Pc(Fe/Co)	10.7	84.11		0.1 M KOH	0.84	5.23	2019 [6]
Fe-NC	0.45	614		0.5 M H_2SO_4	0.85	4.1	2017 [7]
Zn/CoNC	0.47	1343	2.46	0.1 M $HClO_4$	0.796	6.0	2019 [8]
(CM+PANI)-Fe-C	0.2 at%	1500	meso and micro	0.5 M H_2SO_4	0.80	3.00	2018 [9]
CoFeZn/NC	5.51	827.4	5~18	0.1 M KOH	0.85	6.08	This work

References

1 P. Yin, T. Yao, Y. Wu, L. Zheng, Y. Lin, W. Liu, H. Ju, J. Zhu, X. Hong, Z. Deng, G. Zhou, S. Wei, Y. Li, *Angew. Chem. Int. Ed.*, 2016, **55**, 10800-10805.

2 J. Wang, W. Liu, G. Luo, Z. Li, C. Zhao, H. Zhang, M. Zhu, Q. Xu, X. Wang, C. Zhao, Y. Qu, Z. Yang, T. Yao, Y. Li, Y. Lin, Y. Wu, Y. Li, *Energy Environ. Sci.*, 2018, **11**, 3375-3379.

3 F. Li, G.-F. Han, H.-J. Noh, S.-J. Kim, Y. Lu, H. Y. Jeong, Z. Fu, J.-B. Baek, *Energy Environ. Sci.*, 2018,**11**, 2263-2269.

4 L. Shang, H. Yu, X. Huang, T. Bian, R. Shi, Y. Zhao, G. I. Waterhouse, L. Z. Wu, C. H. Tung, T. Zhang, *Adv. Mater.*, 2016, **28**, 1668-1674.

5 Y. Chen, S. Ji, Y. Wang, J. Dong, W. Chen, Z. Li, R. Shen, L. Zheng, Z. Zhuang, D. Wang, Y. Li, *Angew. Chem. Int. Ed.*, 2017, **56**, 6937-6941.

6 P. M. Usov, S. R. Ahrenholtz, W. A. Maza, B. Stratakes, C. C. Epley, M. C. Kessinger, J. Zhu, A. J. Morris, *J. Mater. Chem. A*, 2016, **4**, 16818-16823.

7 H. Zhang, S. Hwang, M. Wang, Z. Feng, S. Karakalos, L. Luo, Z. Qiao, X. Xie, C. Wang, D. Su, Y. Shao, G. Wu, *J. Am. Chem. Soc.*, 2017, **139**, 14143-14149.

8 Z. Lu, B. Wang, Y. Hu, W. Liu, Y. Zhao, R. Yang, Z. Li, J. Luo, B. Chi, Z. Jiang, M. Li, S. Mu, S. Liao, J. Zhang, X. Sun, *Angew. Chem. Int. Ed.*, 2019, **58**, 2648-2652.

9 L. L. Feng, G. Yu, Y. Wu, G. D. Li, H. Li, Y. Sun, T. Asefa, W. Chen, X. Zou, *J. Am. Chem. Soc.*, 2015, **137**, 14023-14026.